scientific reports

Check for updates

OPEN

Magnitude determination for earthquake early warning using *P*-alert low-cost sensors during 2024 Mw7.4 Hualien, Taiwan earthquake

Yueh-Ho Lin[1] & Yih-Min Wu[1,2]✉

Magnitude determination in earthquake early warning (EEW) systems remains a significant challenge. On April 2, 2024, a Mw 7.4 earthquake struck Taiwan. The Central Weather Administration (CWA) EEW system estimated the magnitude at 6.8 within 15 s, resulting in no alerts for the Taipei metropolitan region, which experienced an intensity level of 5 lower (PGV ≥ 15 cm/s) on the CWA's intensity scale. The lack of warning alerts sparked widespread complaints, highlighting concerns over the effectiveness of the current EEW system. This study compares the parameter cumulative absolute absement (CAA) with the currently used parameters — the peak vertical displacement (Pd) and the average period (τ_c) — for quick magnitude estimation of the April 2, 2024, earthquake using low-cost sensors. Results indicate that Pd provides closer estimates of the CWA final M_L but carries higher uncertainty. Conversely, CAA yields more stable estimates. Notably, the northward rupture of this earthquake caused overestimation when only northern stations were used and underestimation with only southern stations, underscoring the critical importance of proper station distribution. Interestingly, τ_c demonstrates less sensitivity to rupture directionality, suggesting its potential robustness in such scenarios. These findings underscore optimizing parameter selection and station configuration for robust EEW, enabling rapid magnitude estimation to significantly reduce losses.

Keywords Earthquake, Earthquake Early Warning, Magnitude Estimation, Low-cost Sensors

Taiwan situated at the convergent boundary between the Philippine Sea Plate and the Eurasian Plate. This region is characterized by complex tectonic interactions, which make Taiwan highly susceptible to frequent and destructive earthquakes, often causing significant loss of life and extensive property damage. Over the years, the region has endured numerous catastrophic seismic events (Fig. 1). For example, on September 20, 1999, the Chi-Chi M_W 7.6 earthquake struck central Taiwan, resulting in 2,456 fatalities, 11,306 injuries, and $4 billion in property damage [1–3]. The 2016 Meinong Mw 6.4 earthquake occurred on February 5 in southwestern Taiwan, causing 117 fatalities, 504 injuries, 141 houses destroyed, and 162 houses damaged [4]. The 2018 Hualien Mw 6.4 earthquake struck eastern Taiwan on February 6, leading to 17 fatalities, 289 injuries, and the destruction of four buildings [5]. Similarly, the 2024 Hualien Mw 7.4 earthquake resulted in 21 fatalities (includes 3 missing), 1,155 injuries, and severe transportation disruptions [6], with most of the damage caused by landslides and falling rocks [7]. These events highlight the urgent need for effective mitigation strategies to reduce seismic risks and enhance resilience.

One of the most promising approaches for reducing the risks posed by damage earthquakes is the implementation of Earthquake Early Warning (EEW) system. These systems have been extensively tested and adopted in various countries [8–11]. By providing valuable seconds of warning before strong seismic waves reach populated areas, the EEW system can help protect lives and reduce damage by enabling timely responses such as halting trains, stopping elevators, and issuing public safety warnings.

Taiwan has been at the forefront of EEW system development for over 30 years and stands as one of leaders in its application [12–17]. The current EEW system, which utilizes the Earthworm Based Earthquake Alarm Reporting (eBEAR) system, has been in operation for around a decade in Central Weather Administration (CWA) [17,18]. The eBEAR system delivers EEW messages via the internet, public warning systems, and television broadcasts to the public, and typically issue alerts within approximately 20 s after an earthquake occurs [18]. It leverages real-time data from a seismic network to rapidly detect and analyze seismic activity, issuing warnings within seconds of

[1]Department of Geosciences, National Taiwan University, No. 1, Section 4, Roosevelt Road, Taipei 10617, Taiwan. [2]Institute of Earth Sciences, Academia Sinica, Taipei 11529, Taiwan. ✉email: drymwu@ntu.edu.tw

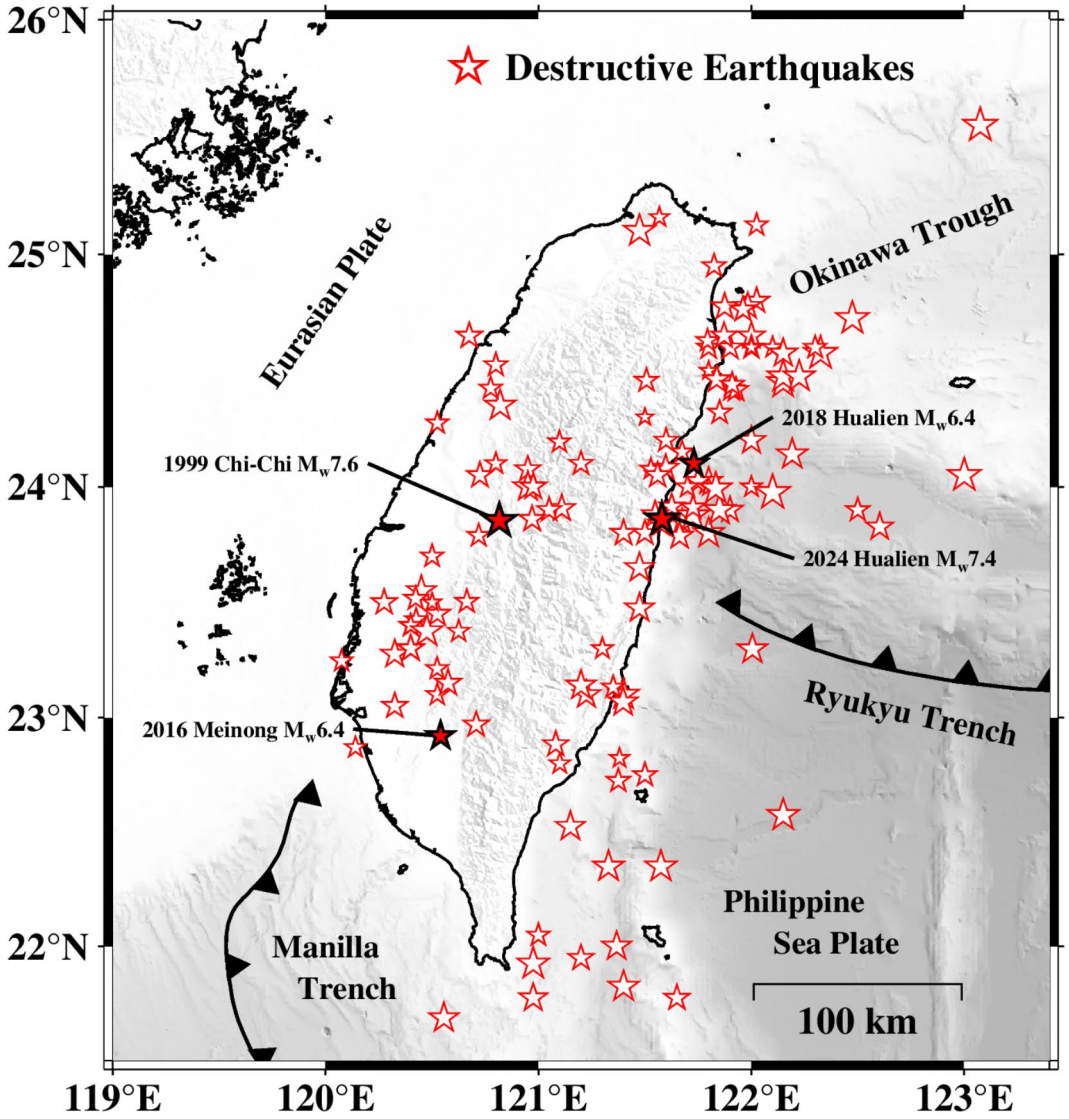

Fig. 1. Tectonics of Taiwan. The red stars show the distribution of epicenters of destructive earthquakes listed by the CWA (https://scweb.cwa.gov.tw/zh-tw/page/disaster/5) since 1900 and the solid red stars indicate that they resulted in over 10 fatalities, following the September 20, 1999, Chi-Chi earthquake.

a damage earthquake occurrence. After detecting the initial P-wave, the system quickly generates earthquake information, such as hypocenter and magnitude. The peak ground acceleration (PGA) is calculated via the ground motion prediction equation (GMPE) of Hsiao [15]. These values are then used by the CWA's new intensity scale to determine the intensity in each region, which dictates whether a warning message should be issued.

On April 2, 2024, eastern Taiwan was struck by an earthquake that caused significant damage in Hualien, resulting in 21 fatalities [6]. Only one person was killed by a building collapse, while most casualties occurred due to coseismic landslides, which were predominantly concentrated in areas with PGA exceeding 250 gal [7]. The CWA EEW system successfully issued alerts; however, the Taipei metropolitan region, where most of the publication in this area resides, notably lacked national-level alerts [19]. This was due to the EEW system estimating a PGA of less than 25 gal in the Taipei metropolitan region, despite ground shaking exceeding 80 gal across most of northern Taiwan and causing damage (Fig. 2). This absence of an alert has sparked considerable public debate and caused serious transportation disruptions, most notably a derailment incident on the Taipei Metro Rapid Transit, further highlighting the impact of the event. As the earthquake occurred during peak commuting hours, it resulted in substantial transit delays and temporary suspension of metro services. Fortunately, there were no reported casualties at the time of the incident. While the main reason might be the northward rupture of the earthquake (Fig. 2) [20], the CWA's underestimation of the magnitude is also a contributing factor. The United States Geological Survey (USGS) reported the earthquake's M_W as 7.4 [21], while the CWA reported a M_L of 7.2. The USGS slip distribution also indicates a predominantly N26°E unilateral rupture for this event (Fig. 2). However, the initial report from the EEW system of the CWA indicated a magnitude of only 6.2 at 9 s, which later

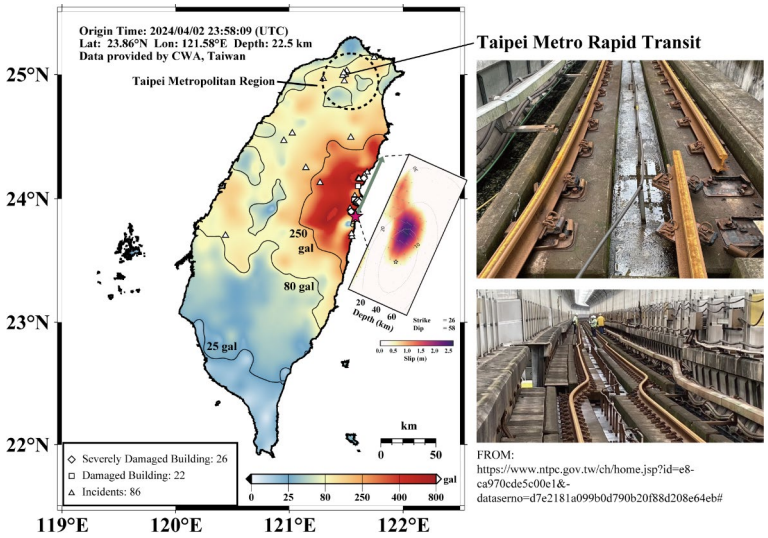

Fig. 2. PGA shakemap [22] with the damage distribution reported by New Taipei City Government [23] and National Science and Technology Center for Disaster Reduction [24]. Annotations highlight the Taipei metropolitan region and disruptions to the MRT. The red star indicates the epicenter of the M_W 7.4 earthquake in Hualien County. The arrow indicates the main rupture direction, and the cross-section shows the slip distribution provided by the USGS [21].

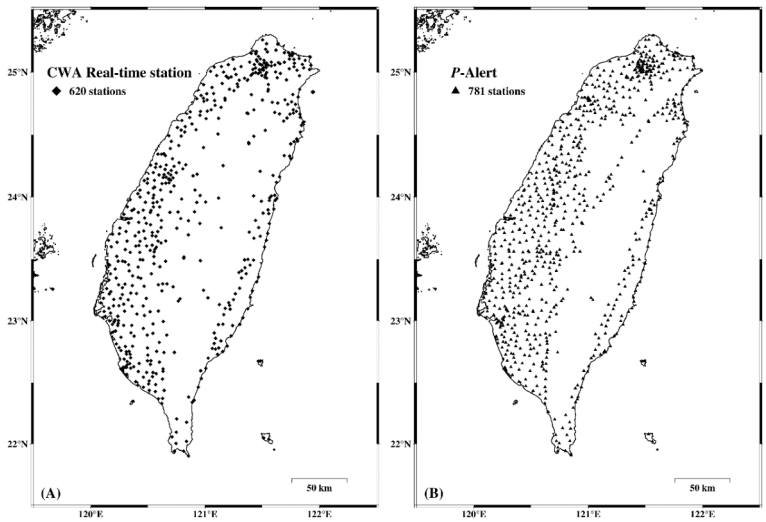

Fig. 3. (**A**) Station distribution of CWA real-time EEW system. (**B**) Station distribution for *P*-Alert network in Taiwan.

increased to 6.8 at 15 s after the earthquake occurrence. Ultimately, the M_L was determined to be approximately 7.2, highlighting that the initial fast-report estimates were underestimated.

Song et al. [25] have previously evaluated the performance of the eBEAR system during the April 2, 2024, Hualien earthquake. The study highlighted the system's challenges in delivering timely alerts, enhancements and better data integration to improve real-time response for seismic events in Taiwan. The eBEAR system [17] plays a crucial role in Taiwan's EEW infrastructure by processing data from a wide array of seismic stations distributed across the region (Fig. 3A). Although this network has been effective, the remain challenges in quickly and accurately estimating magnitude, especially during complex seismic events. In addition to this, Taiwan has developed other complementary dense seismic monitoring networks, such as the *P*-Alert network. *P*-Alert seismic network funded by the National Science and Technology Council of Taiwan and developed by National Taiwan University since 2010 [26]. *P*-Alert instruments began in the Hualien area [27], a region frequently affected by earthquakes, and were followed by the installation of 781 instruments across Taiwan, spaced every 5 km (Fig. 3B). Most are situated in schools, ensuring reliable power and internet connections. The effectiveness of the *P*-Alert network in various seismic events has been demonstrated [4,28,29]. However, the *P*-Alert network has primarily been utilized to generate shakemaps for emergency response purposes [30–32], with limited focus on

detailed studies related to earthquake magnitude estimation. Therefore, this study aims to leverage data from the *P*-Alert network to investigate magnitude estimation, providing an alternative enhancement to Taiwan's EEW capabilities.

For magnitude estimation, the eBEAR system relies on the vertical peak displacement (Pd) from initial P-waves to determine magnitude (M_{Pd}), and approach based on the formula proposed by Hsiao et al. [33] Mittal et al. [32] highlighted that the accuracy of magnitude estimation in EEW is one of the key challenges for providing reliable alerts and appropriate responses. The EEW system relies on several key parameters to rapidly assess an earthquake's initial magnitude and potential impact. Current methodologies for estimating earthquake magnitude involve analyzing the frequency (period) and the amplitude parameters of the initial seismic signals [34–36]. These approaches establish regression relationships between these parameters and the initial signals following the arrival of P-waves. As the period parameters, such as the average period (τ_c) and the maximum dominant ground motion period (τ_p^{max}), demonstrate high sensitivity to the final magnitude and are relatively resistant to seismic wave attenuation over distance [34–41]. In terms of the amplitude parameters, Wu and Zhao [36] proposed the Pd method, which correlates the peak amplitude within the initial 3 s following P-wave arrival with the earthquake magnitude. While the Pd parameter has been a stable in EEW system for magnitude estimation [36,42], it only catches a single peak value from the initial P-waves might cause limitations and overlooking valuable information. Other parameters incorporate not only the amplitude of the motion but also its duration and waveform characteristic, the cumulative absolute velocity (CAV), was developed in 1988 and applied in various contexts and applications [43–46]. The CAV approach offers a more holistic perspective by integrating data over time. Huang and Wu [47] explored the effectiveness of multiple initial ground motion parameters and found CAA exhibited a particularly strong correlation with earthquake magnitude.

Wu et al. [48] proposed the CAA parameter as an effective approach for estimating magnitude. Wu [49] applied this method with the *P*-Alert network. Therefore, this study aims to utilize the *P*-Alert network to analyze the CAA parameter and compare it with the traditional Pd parameter and τ_c parameter to explore potential improvements in the EEW system for accurately determining the magnitude the April 2, 2024, Hualien earthquake. By employing playback technology to reconstruct the real-time conditions of the earthquake, this study validates the performance of these parameters in simulating the actual early warning process, providing a comprehensive evaluation of their reliability and effectiveness.

Data and analysis

In this study, we analyzed the signals recorded during the April 2, 2024, Hualien earthquake using data from the *P*-Alert network system (Fig. 3). The *P*-Alert seismic network consists of 781 low-cost MEMS-based acceleration sensors distributed across Taiwan. Each sensor provides real-time, three-component acceleration signals with a sampling rate of 100 samples per second, 16-bit resolution and a ± 2 g recording range [18]. To reconstruct the actual conditions during the earthquake, we used all available records, including those with data gaps, provided the necessary parameters could be calculated from the station's record.

During the analysis process, the vertical component of each record was processed using Allen's algorithm [50] for automatic P-wave detection. Wu and Kanamori [51] proposed the Pd method in Earthquake Early warning. The Pd parameter represents the peak vertical displacement following the arrival of P waves and is extracted from the vertical component by applying a high-pass filter to the displacement signals at 0.075 Hz.

According to Wu and Teng [45], CAA is defined as

$$CAA = \int_{T_p}^{T_{p+i}} \sqrt{Dv^2 + Dn^2 + De^2}\,dt \tag{1}$$

where D*v* corresponds to the vertical displacement, D*n* to the north–south displacement, and D*e* to the north–south displacement. P denotes the arrival of the P-waves, and *i* indicates the subsequent time interval.

As τ_c, Kanamori [35] introduces the period parameter,

$$\tau_c = \frac{2\pi}{\sqrt{r}} \tag{2}$$

where r is given by $[\int_0^{\tau_0} \dot{u}^2(t)dt]/[\int_0^{\tau_0} u^2(t)dt]$. In this equation, u(t) represents the ground-motion displacement, and τ_0 is the duration of record used. Additionally, this study adopts the empirical regression formula for τ_c proposed by Wu et al. [52] for magnitude determination (M_{τ_c}).

In this study, we utilized three parameters, CAA, Pd and τ_c, to estimate earthquake magnitude. Both the CAA and Pd (Fig. 4) are computed for varying time windows ranging from 2 to 5 s [49]. The relationships for magnitude estimation using CAA and Pd with following regression Eqs. [36]:

$$\log(Pd) = a * \log(R) + b * M_w + c \tag{3}$$

$$\log(CAA) = a * \log(R) + b * M_w + c \tag{4}$$

where R is the hypocentral distance in km, and the coefficients a, b, c are the coefficients provided in Table 1 [49].

The equation revealed that hypocentral distance plays a crucial role in magnitude estimation. Notably, the real-time location from the *P*-Alert seismic network closely aligns with the final hypocenter from the CWA in Taiwan (Fig. 5). However, as indicated by the grey area in Fig. 5, earthquake location estimates inherently exhibit uncertainty and variability, especially during the initial seconds of seismic event. The dynamic location

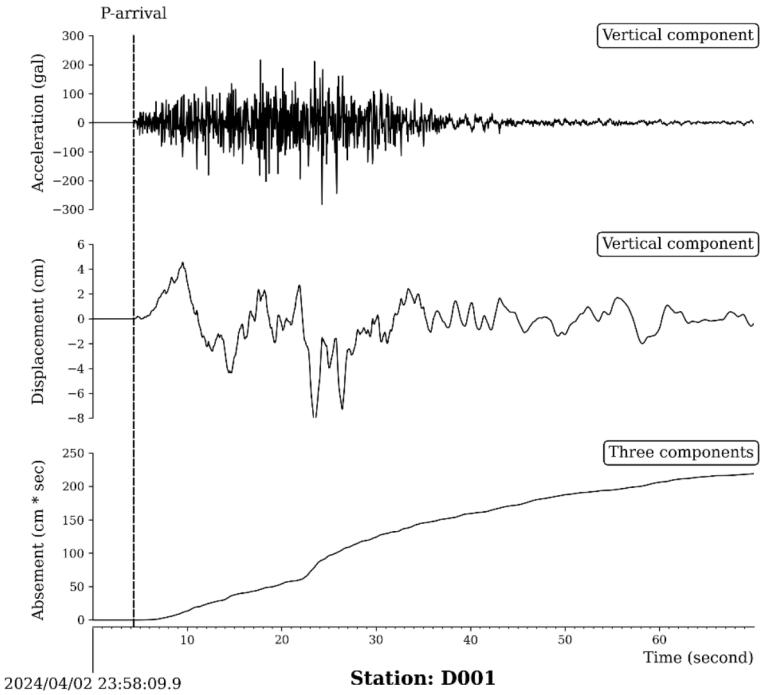

Fig. 4. Acceleration records, the filtered vertical displacement and CAA at the station D001 (Δ = 15.8 km). The vertical dashed line is drawn as the P arrival.

Parameter	Window(s)	a	b	c	sdv
CAA	2	− 1.007	0.191	− 0.341	0.277
	3	− 1.278	0.298	− 0.244	0.274
	4	− 1.416	0.347	− 0.104	0.263
	5	− 1.465	0.36	0.063	0.258
Pd	2	− 1.072	0.197	− 0.541	0.347
	3	− 1.293	0.266	− 0.469	0.316
	4	− 1.425	0.308	− 0.418	0.302
	5	− 1.449	0.335	− 0.448	0.305

Table 1. Values of the coefficients *a*, *b*, and *c* used in this study.

data provided by the *P*-Alert network enable continuous adjustment of the hypocentral distance in real-time, reflecting the evolving understanding of the earthquake's location as it unfolds. This study will utilize real-time location data from the *P*-Alert seismic network.

Results and discussion

As mentioned previously, time windows ranging from 2 to 5 s were employed for magnitude estimation in this study. Figure 6 presents the playback analysis, it reveals the behavior of M_{Pd}, M_{τ_c} and M_{CAA} parameters in estimating the magnitude during the April 2, 2024, Hualien earthquake. Initial magnitude estimates began approximately 5 s after the earthquake's onset. At around 8 s, the M_{Pd} estimate was 6.9, while M_{CAA} is 6.3 and M_{τ_c} is 6.8. By 13 s, M_{Pd} had increased to approximately 7.1, whereas M_{CAA} reached a higher value of 6.9, and $M_{\tau c}$ briefly decreased to 6.8. Despite these variations, all three parameters ultimately converged closely on the final M_L of CWA report by 35 s after the origin-time, with M_{Pd} finalizing at 7.2, M_{CAA} at 7.3, and M_{τ_c} settled at 7.1. This final convergence suggests that, while early estimation trends differed, both Pd, τ_c and CAA provided reliable magnitude approximations by the end of the playback period.

However, it should be noted that although these proposed methods outperformed the current CWA EEW estimates, the final estimated magnitudes remained slightly lower than M_W 7.4 reported by the USGS. Even seemingly minor discrepancies can significantly affect the EEW system, potentially influencing whether an alert is issued or altering predicted ground-motion intensities.

Contrary to this study, the CWA EEW system reported a magnitude of only 6.2 at 9 s and 6.8 at 15 s after the earthquake. This significant underestimation can be primarily attributed to location errors in the early stages of detection (Fig. 5). Accurate earthquake location is crucial for magnitude estimation, as it directly affects

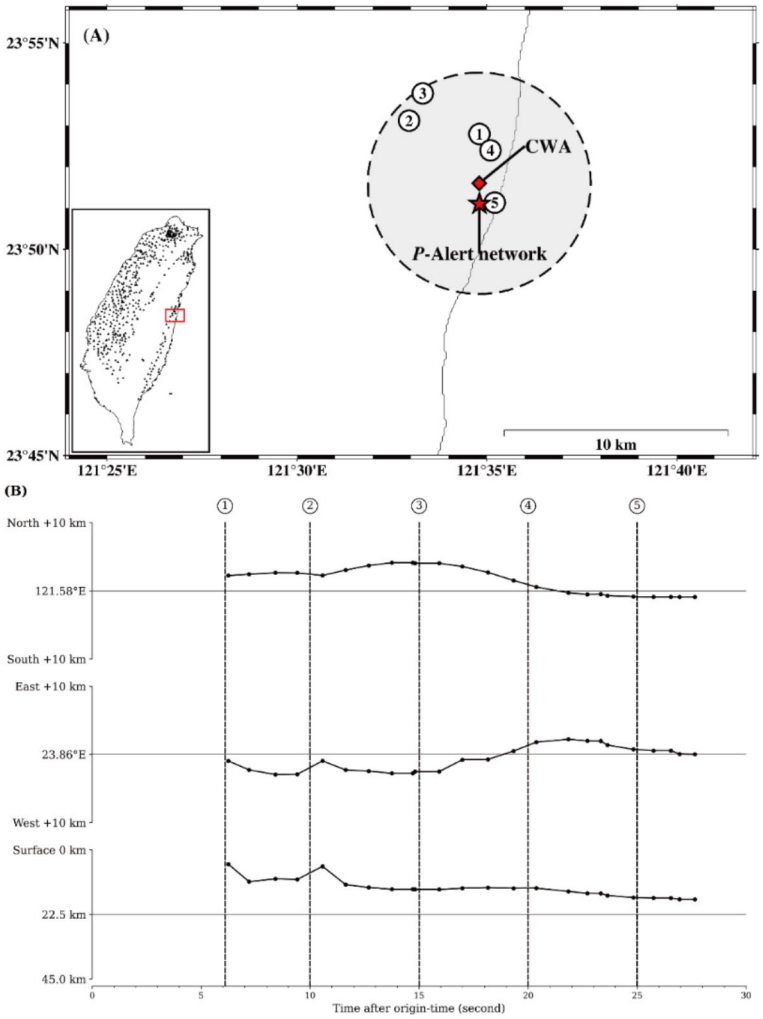

Fig. 5. (**A**) Show the triggered stations of the *P*-Alert network during the April 2, 2024, Hualien earthquake, which are the stations used in this study. The *P*-Alert network and the CWA location results are displayed. The grey-shaded area represents the variation of epicenter by the *P*-Alert network, centered around the CWA-reported epicenter. The circle markers indicate the dynamic positioning process. (**B**) Comparing the dynamic location results from the *P*-Alert network with the CWA location results.

the calculation of hypocentral distances. In addition to location errors, unilateral rupture propagation caused asymmetrical seismic wave distribution, which further complicated accurate distance calculations and led to an underestimation of the earthquake magnitude. Critically, this underestimation resulted in the loss of a warning message.

Moreover, the finite-fault model from the USGS indicates that the 2024 Hualien earthquake ruptured over approximately 50 km within about 45 s [21]. Assuming a relatively uniform rupture propagation, only about 23–28 km of the fault would have ruptured within the first 9 s. This implies that the moment release at that time corresponded to a magnitude of around 6.7–6.8, which aligns well with the M_{Pd} and M_{τ_c}. Although M_{CAA} was slightly lower, its standard deviation remained lower than that of M_{Pd} and M_{τ_c} during the early stages, suggesting that CAA may still provide valuable and stable reference information in the initial seconds of rupture. This finding underscores that the rupture duration is import in magnitude estimation, especially for large earthquakes. However, due to the limited time window in EEW systems, incorporating source duration remains a significant challenge.

The April 2, 2024, the Hualien earthquake exhibited a northward rupture direction, presenting an additional challenge for the EEW system. To investigate this effect, we divided the region into northern and southern sectors relative to the epicenter and conducted magnitude estimations for each sector (Fig. 7). This simple division was adopted because the station distribution in the affected area happened to align well with the rupture direction, allowing for a meaningful comparison of directivity effects. The result revealed that the magnitude estimated in the southern region was significantly underestimated compared to the northern region. This observation highlights the impact of ruptured directivity on EEW performance. The rupture directivity effect poses a challenge for EEW, as it can lead to inconsistent magnitude estimations across different areas, potentially affecting the accuracy and timeliness of warnings. However, several methods have been proposed to address

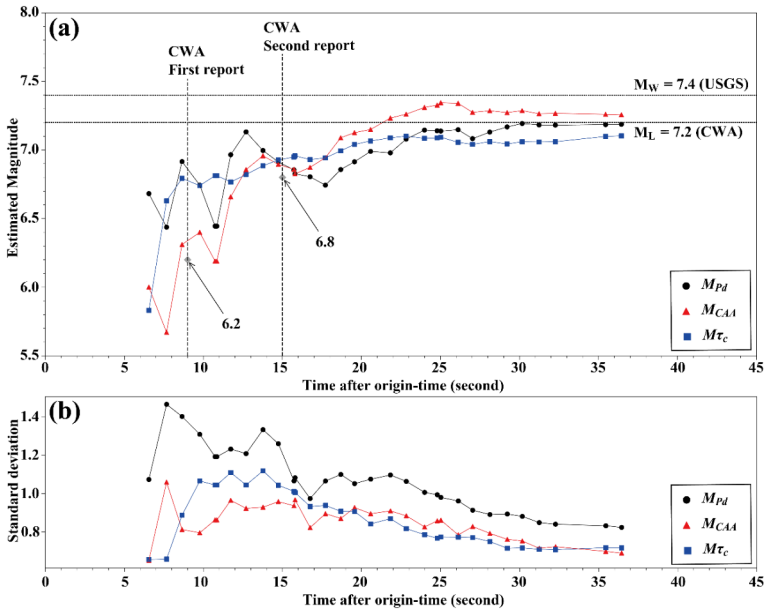

Fig. 6. Playback results of magnitude estimation and their standard deviation using Pd, CAA and τ_c. (**a**) Evolution of magnitude estimates over time during the playback of the April 2, 2024, Hualien earthquake. The blue, red and black indicate estimates derived from Pd, CAA and τ_c, respectively. The horizontal dashed line represents the final local magnitude reported by the CWA, and the horizontal solid line corresponds to the moment magnitude reported by the USGS. The two vertical dashed lines indicate the times at which the CWA EEW system issued alerts. (**b**) Corresponding standard deviations of magnitude estimates.

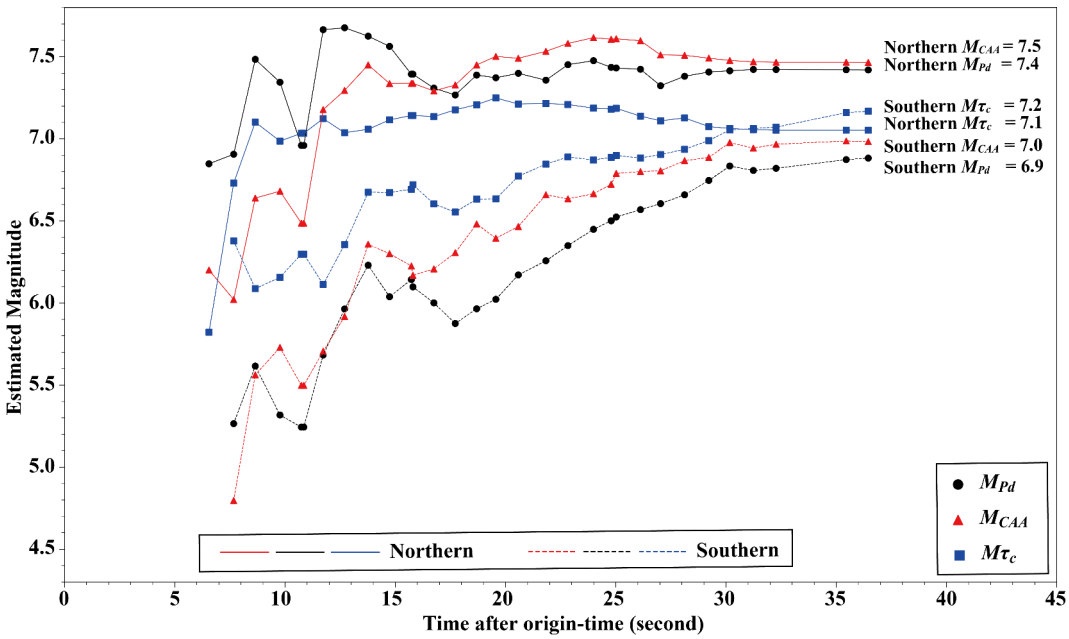

Fig. 7. Comparison of magnitude estimations based on M_{Pd}, M_{CAA} and $M_{\tau c}$ parameters, with the stations divided into northern and southern regions from epicenter.

this issue. For instance, the ShakingAlarm approach by Yang et al. [53] and data-driven EEW methods like Japan Meteorological Agency PLUM [54] show potential for mitigating this effect. Additionally, the method proposed by Jan et al. [55] offers another promising solution to this problem.

Furthermore, the significance of station distribution cannot be overstated, as it plays a vital role in the accuracy of traditional magnitude determination methods. A well-distributed network of seismic stations ensures that data from various locations can be integrated, providing a more comprehensive picture of the earthquake's characteristics. This spatial coverage is particularly important for evaluating how rupture directivity

affects the early warning parameter. A uniformly distributed network also helps reduce the estimation bias when stations are unevenly positioned relative to the rupture direction. Interestingly, in our analysis, τ_c was found to be less sensitive to rupture directivity compared to Pd and CAA, as the estimations derived from τ_c stabilized more consistently across the northern and southern sectors. This finding suggests that τ_c may offer a more robust approach in addressing the challenges posed by rupture directivity warranting further exploration as a potential enhancement to EEW systems. This approach enhances the robustness of the EEW system, ensuring that warnings are timely and accurate across different regions.

Conclusions

The underestimation of earthquake magnitude significantly impacts the effectiveness of EEW systems. In this study, we applied the CAA parameters to evaluate the magnitude of the April 2, 2024, Hualien earthquake. The analysis revealed that while M_{Pd} provided estimates closer to the final M_L reported by the CWA, it lacked stability during the estimation process. In contrast, the M_{CAA} approach demonstrated greater stability, as evidenced by its lower standard deviation, resulting in more consistent magnitude estimates in the critical early seconds following an earthquake. This stability is essential for the prompt and accurate functioning of EEW systems.

Furthermore, in real-time earthquake early warning applications, location estimates are inherently dynamic, especially during the initial seconds of seismic events. Unlike retrospective analyses that rely on final location result, real-time estimates continuously evolve, leading to fluctuations in hypocentral distances and affecting subsequent magnitude calculations. This variability presents a challenge for real-time systems; each update in location data leads to adjustments in magnitude estimates, underscoring the importance of enhancing real-time update mechanisms to maintain alert accuracy.

Due to the northward rupture of the April 2 earthquake, there are differences in magnitude estimates between the northern and southern regions, highlighting the importance of the distribution of stations. Optimizing the station's distribution is crucial for enhancing the overall performance of EEW system and ensuring that communities receive accurate and timely warnings. Additionally, data loss and instability can lead to estimation errors and localization inaccuracies, further impacting the reliability of the magnitude estimation. These challenges underscore the need for continued research and improvement in EEW methodologies.

While the CAA parameter offers stability within its optimal time window and the Pd parameter provides accuracy, neither is sufficient on its own to fully optimize EEW system performance. Notably, the τ_c parameter demonstrated lower sensitivity to rupture directivity and maintained consistent performance across regions with varying station coverage. This robust positions τ_c as a promising complement to existing methodologies, particularly in addressing the challenges posed by rupture directivity. Effectively tackling the complexities of station distribution, data losses, and rupture directivity is critical for advancing EEW systems and enhancing public safety and preparedness.

Data availability

All *P*-Alert strong-motion records used in this study are publicly available and can be downloaded from this website https://palert.earth.sinica.edu.tw/database.

Received: 24 January 2025; Accepted: 7 April 2025
Published online: 12 April 2025

References

1. Shin, T. C. & Teng, T. L. An overview of the 1999 Chi-Chi, Taiwan earthquake. *Bull. Seism. Soc. Am.* **91**, 895–913. https://doi.org/10.1785/0120000738 (2001).
2. Wu, Y. M., Hsiao, N. C. & Teng, T. L. Relationships between strong ground motion peak values and seismic loss during the 1999 Chi-Chi, Taiwan earthquake. *Nat. Hazard.* **32**, 357–373. https://doi.org/10.1023/B:NHAZ.0000035550.36929.d0 (2004).
3. Shih, D. C. F. & Wu, Y. M. Exploring building vibration dynamics in the wake of the Chi-Chi earthquake: Implications for natural hazard preparedness. *Nat. Hazard.* **120**, 12851–12867. https://doi.org/10.1007/s11069-024-06721-y (2024).
4. Wu, Y. M. et al. Performance of a low-cost earthquake early warning system (P-Alert) during the 2016 ML 6.4 Meinong (Taiwan) earthquake. *Seism. Res. Lett.* **87**, 1050–1059. https://doi.org/10.1785/0220160058 (2016).
5. Ma, K. F. & Wu, Y. M. Preface to the Focus Section on the 6 February 2018 Mw 6.4 Hualien, Taiwan, earthquake. *Seism. Res. Lett.* **90**, 15–18. https://doi.org/10.1785/0220180356 (2018).
6. Wikipedia. 2024 Hualien Earthquake, https://en.wikipedia.org/wiki/2024_Hualien_earthquake (2024). Accessed January 7 2025.
7. Chang, J. M., Chao, W. A., Yang, C. M. & Huang, M. W. Coseismic and subsequent landslides of the 2024 Hualien earthquake (M7.2) on April 3 in Taiwan. *Landslides* **21**, 2591–2595. https://doi.org/10.1007/s10346-024-02312-x (2024).
8. Alcik, H., Ozel, O., Apaydin, N. & Erdik, M. A study on warning algorithms for Istanbul earthquake early warning system. *Geophys. Res. Lett.* **36**, L00B05. https://doi.org/10.1029/2008GL036659 (2009).
9. Lee, W. H. K. & Wu, Y. M. Earthquake Monitoring and Early Warning Systems. In *Encyclopedia of Complexity and Systems Science* (ed. Meyers, R. A.) 2496–2530 (Springer, New York, 2009).
10. Nakamura, Y., Saita, J. & Sato, T. On an earthquake early warning system (EEW) and its applications. *Soil Dyn. Earthquake Eng.* **31**, 127–136. https://doi.org/10.1016/j.soildyn.2010.04.012 (2011).
11. Satriano, C., Wu, Y. M., Zollo, A. & Kanamori, H. Earthquake early warning: Concepts, methods and physical grounds. *Soil Dyn. Earthq. Eng.* **31**, 106–118. https://doi.org/10.1016/j.soildyn.2010.07.007 (2011).
12. Wu, Y. M., Shin, T. C. & Tsai, Y. B. Quick and reliable determination of magnitude for seismic early warning. *Bull. Seism. Soc. Am.* **88**, 1254–1259. https://doi.org/10.1785/BSSA0880051254 (1998).
13. Wu, Y. M. et al. Development of an integrated seismic early warning system in Taiwan. *Terr. Atmos. Ocean. Sci.* **10**, 719–736. https://doi.org/10.3319/TAO.1999.10.4.719(T) (1999).
14. Wu, Y. M. & Teng, T. L. A virtual subnetwork approach to earthquake early warning. *Bull. Seism. Soc. Am.* **92**, 2008–2018. https://doi.org/10.1785/0120010217 (2002).
15. Hsiao, N. C. The application of real-time strong-motion observations on the earthquake early warning in Taiwan (in Chinese with English abstract), Ph.D. thesis, 178 (Inst. of Geophys. Natl. Cent. Univ., Taiwan. 2007).

16. Hsiao, N. C., Wu, Y. M., Shin, T. C., Zhao, L. & Teng, T. L. Development of earthquake early warning system in Taiwan. *Geophys. Res. Lett.* **36**, L00B02. https://doi.org/10.1029/2008GL036596 (2009).
17. Chen, D. Y., Hsiao, N. C. & Wu, Y. M. The Earthworm based earthquake alarm reporting system in Taiwan. *Bull. Seism. Soc. Am.* **105**, 568–579. https://doi.org/10.1785/0120140147 (2015).
18. Wu, Y. M., Mittal, H., Chen, D. Y., Hsu, T. Y. & Lin, P. Y. Earthquake early warning systems in Taiwan: Current status. *J. Geol. Soc. India* **97**, 1525–1532. https://doi.org/10.1007/s12594-021-1909-6 (2021).
19. CWA. Central Weather Administration News. https://www.cwa.gov.tw/Data/service/Newsbb/CH/Newsbb_20240403225329.pdf. (2024a). Accessed 7 January 2025.
20. Cheloni, D., Famiglietti, N. A., Caputo, R., Tolomei, C. & Vicari, A. A composite fault model for the 2024 MW 7.4 Hualien earthquake sequence in eastern Taiwan inferred from GNSS and InSAR data. *Geophys. Res. Lett.* **51**, e2024GL110255. https://doi.org/10.1029/2024GL110255 (2024).
21. USGS. M 7.4 - 15 km S of Hualien City, Taiwan, https://earthquake.usgs.gov/earthquakes/eventpage/us7000m9g4/executive. (2024). Accessed July 31 2024.
22. CWA. Central Weather Administration earthquake Report. https://scweb.cwa.gov.tw/en-us/earthquake/data (2024b). Accessed 7 January 2025.
23. NTCP. New Taipei City Government News Report. https://www.ntpc.gov.tw/ch/home.jsp?id=e8ca970cde5c00e1&dataserno=d7e2181a099b0d790b20f88d208e64eb# (2024). Accessed January 7 2025.
24. NCDR. National Science and Technology Center for Disaster Reduction Report. https://den1.ncdr.nat.gov.tw/1330/1334/1335/17836/17849/ (2024). Accessed January 7 2025.
25. Song, G.Y. et al. Application of SeisComP at the Central Weather Administration (CWA) for Earthquake Monitoring and Early Warning: A Case Study of the 2024 ML 7.2 Hualien, Taiwan, Earthquake Sequence. In *EGU General Assembly Conference Abstracts*, 2025-May, EGU25-5275. 10.5194/egusphere-egu25-5275 (2025).
26. Wu, Y. M. et al. A high-density seismic network for earthquake early warning in taiwan based on low cost sensors. *Seism. Res. Lett.* **84**, 1048–1054. https://doi.org/10.1785/0220130085 (2013).
27. Wu, Y.-M. & Lin, T.-L. A Test of Earthquake Early Warning System Using Low Cost Accelerometer in Hualien, Taiwan. In *Early Warning for Geological Disasters: Scientific Methods and Current Practice* (eds Wenzel, F. & Zschau, J.) 253–261 (Springer Berlin Heidelberg, Berlin, Heidelberg, 2014). https://doi.org/10.1007/978-3-642-12233-0_13.
28. Wu, Y. M. et al. Performance of a low-cost earthquake early warning system (P-Alert) and shake map production during the 2018 Mw 6.4 Hualien, Taiwan earthquake. *Seism. Res. Lett.* **90**, 19–29. https://doi.org/10.1785/0220180170 (2019).
29. Wu, Y. M. Progress on development of an earthquake early warning system using low-cost sensors. *Pure Appl. Geophys.* **172**, 2343–2351. https://doi.org/10.1007/s00024-014-0933-5 (2015).
30. Yang, B. M., Mittal, H. & Wu, Y. M. Real-time production of PGA, PGV, intensity, and Sa Shakemaps using dense MEMS-based sensors in Taiwan. *Sensors* **21**, 943. https://doi.org/10.3390/s21030943 (2021).
31. Mittal, H., Yang, B. M., Tseng, T. L. & Wu, Y. M. Importance of real-time PGV in terms of lead-time and shakemaps: Results using 2018 ML 6.2 & 2019 ML 6.3 Hualien Taiwan earthquakes. *J. Asian Earth Sci.* **220**, 104936. https://doi.org/10.1016/j.jseaes.2021.104936 (2021).
32. Mittal, H., Yang, B. M. & Wu, Y. M. Progress on the earthquake early warning and shakemaps system using low-cost sensors in Taiwan. *Geosci. Lett.* **9**, 42. https://doi.org/10.1186/s40562-022-00251-w (2022).
33. Hsiao, N. C. et al. A new prototype system for earthquake early warning in Taiwan. *Soil Dyn. Earthquake Eng.* **31**, 201–208. https://doi.org/10.1016/j.soildyn.2010.01.008 (2011).
34. Nakamura, Y. On the urgent earthquake detection and alarm system (UrEDAS). *Proc. of the 9th World Conference on Earthquake Engineering* **7**, 673–678 (1988).
35. Kanamori, H. Real-time seismology and earthquake damage mitigation. *Annu. Rev. Earth Planet. Sci.* **33**, 195–214. https://doi.org/10.1146/annurev.earth.33.092203.122626 (2005).
36. Wu, Y. M. & Zhao, L. Magnitude estimation using the first three seconds P-wave amplitude in earthquake early warning. *Geophys. Res. Lett.* **33**, 16. https://doi.org/10.1029/2006GL026871 (2006).
37. Wu, Y. M. & Kanamori, H. Rapid assessment of damage potential of earthquakes in Taiwan from the beginning of P waves. *Bull. Seism. Soc. Am.* **95**, 1181–1185. https://doi.org/10.1785/0120040193 (2005).
38. Wu, Y. M., Kanamori, H., Allen, R. M. & Hauksson, E. Determination of earthquake early warning parameters, τ_c and Pd, for southern California. *Geophys. J. Int.* **170**, 711–717. https://doi.org/10.1111/j.1365-246X.2007.03430.x (2007).
39. Allen, R. M. & Kanamori, H. The potential for earthquake early warning in southern California. *Science* **300**, 786–789. https://doi.org/10.1126/science.1080912 (2003).
40. Yamada, M. & Mori, J. Using τ_c to estimate magnitude for earthquake early warning and effects of near-field terms. *J. Geophys. Res.* **114**, B05301. https://doi.org/10.1029/2008JB006080 (2009).
41. Zollo, A., Amoroso, O., Lancieri, M., Wu, Y. M. & Kanamori, H. A threshold-based earthquake early warning using dense accelerometer networks. *Geophys. J. Int.* **183**, 963–974. https://doi.org/10.1111/j.1365-246X.2010.04765.x (2010).
42. Zollo, A., Lancieri, M. & Nielsen, S. Earthquake magnitude estimation from peak amplitudes of very early seismic signals on strong motion records. *Geophys. Res. Lett.* **33**, L23312. https://doi.org/10.1029/2006GL027795 (2006).
43. EPRI A criterion for determining exceedance of the operating basis earthquake. Electric Power Research Institute, Palo Alto, CA, prepared by Jack R. Benjamin and Associates, Inc., Report No:NP-5930. https://www.osti.gov/biblio/6968267 (1988).
44. Erdik, M. et al. Istanbul earthquake rapid response and the early warning system. *Bull. Earthquake Eng.* **1**, 157–163. https://doi.org/10.1023/A:1024813612271 (2003).
45. Wu, Y. M. & Teng, T. L. Near real-time magnitude determination for large crustal earthquakes. *Tectonophysics* **390**, 205–216. https://doi.org/10.1016/j.tecto.2004.03.029 (2004).
46. Kramer, S. L. & Mitchell, R. A. Ground motion intensity measures for liquefaction hazard evaluation. *Earthq. Spectra* **22**, 413–438. https://doi.org/10.1193/1.2194970 (2006).
47. Huang, H.Y. & Wu, Y.M. Magnitude Estimation and Onsite Earthquake Early Warning using Cumulative Absolute Velocity in Taiwan. EGU General Assembly Conference Abstracts, 2021-April, EGU21-8570. 10.5194/egusphere-egu21-8570 (2021).
48. Wu, Y. M., Mittal, H., Lin, Y. H. & Chang, Y. H. Magnitude determination using cumulative absolute absement for earthquake early warning. *Geosci. Lett.* **10**, 59. https://doi.org/10.1186/s40562-023-00314-6 (2023).
49. Wu, Y.M. Cumulative absolute absement for magnitude determination in earthquake early warning system using low-cost sensors. In EGU General Assembly Conference Abstracts, 2024-Mar, EGU24-2969. 10.5194/egusphere-egu24-2969 (2024).
50. Allen, R. V. Automatic earthquake recognition and timing from single traces. *Bull. Seism. Soc. Am.* **68**, 1521–1532. https://doi.org/10.1785/BSSA0680051521 (1978).
51. Wu, Y. M. & Kanamori, H. Experiment on an onsite early warning method for the Taiwan early warning system. *Bull. Seism. Soc. Am.* **95**, 347–353. https://doi.org/10.1785/0120040097 (2005).
52. Wu, Y. M., Yen, H. Y., Zhao, L., Huang, B. S. & Liang, W. T. Magnitude determination using initial P waves: A single-station approach. *Geophys. Res. Lett.* **33**, L05306. https://doi.org/10.1029/2005GL025395 (2006).
53. Yang, B. M., Huang, T. C. & Wu, Y. M. ShakingAlarm: A non-traditional regional earthquake early warning system based on time-dependent anisotropic peak ground motion attenuation relationships. *Bull. Seism. Soc. Am.* **108**, 1219–1230. https://doi.org/10.1785/0120170105 (2018).

54. Kodera, Y. et al. The propagation of local undamped motion (PLUM) method: A simple and robust seismic wavefield estimation approach for earthquake early warning. *Bull. Seism. Soc. Am.* **108**, 983–1003. https://doi.org/10.1785/0120170085 (2018).
55. Jan, J. C., Huang, H. H., Wu, Y. M., Chen, C. C. & Lin, C. H. Near-real-time estimates on earthquake rupture directivity using near-field ground motion data from a dense low-cost seismic network. *Geophys. Res. Lett.* **45**, 7496–7503. https://doi.org/10.1029/2018GL078262 (2018).

Acknowledgements
The authors gratefully acknowledge the National Science and Technology Council (NSTC), Taiwan with Grant Numbers 113-2740-M-002 -005 and 113-2116-M-002 -014 for sponsoring this study.

Author contributions
Y.H.L. and Y.M. W. wrote the main manuscript text and Y.H.L. prepared figures. All authors reviewed the manuscript.

Funding
This study was supported by the National Science and Technology Council, Taiwan, with Grant Numbers 113-2740-M-002 -005 and 113-2116-M-002 -014.

Declarations

Competing interests
The authors declare no competing interests.

Additional information
Correspondence and requests for materials should be addressed to Y.-M.W.

Reprints and permissions information is available at www.nature.com/reprints.

Publisher's note Springer Nature remains neutral with regard to jurisdictional claims in published maps and institutional affiliations.

Open Access This article is licensed under a Creative Commons Attribution-NonCommercial-NoDerivatives 4.0 International License, which permits any non-commercial use, sharing, distribution and reproduction in any medium or format, as long as you give appropriate credit to the original author(s) and the source, provide a link to the Creative Commons licence, and indicate if you modified the licensed material. You do not have permission under this licence to share adapted material derived from this article or parts of it. The images or other third party material in this article are included in the article's Creative Commons licence, unless indicated otherwise in a credit line to the material. If material is not included in the article's Creative Commons licence and your intended use is not permitted by statutory regulation or exceeds the permitted use, you will need to obtain permission directly from the copyright holder. To view a copy of this licence, visit http://creativecommons.org/licenses/by-nc-nd/4.0/.

© The Author(s) 2025